
MixupE: Understanding and Improving Mixup from Directional Derivative Perspective

Vikas Verma^{1,2}

Sarthak Mittal¹

Wai Hoh Tang⁴

Hieu Pham³

Juho Kannala²

Yoshua Bengio¹

Arno Solin²

Kenji Kawaguchi⁴

¹Universite de Montreal, Mila

²Aalto University, Finland

³Google Brain

⁴National University of Singapore

Abstract

Mixup is a popular data augmentation technique for training deep neural networks where additional samples are generated by linearly interpolating pairs of inputs and their labels. This technique is known to improve the generalization performance in many learning paradigms and applications. In this work, we first analyze Mixup and show that it implicitly regularizes infinitely many directional derivatives of all orders. We then propose a new method to improve Mixup based on the novel insight. To demonstrate the effectiveness of the proposed method, we conduct experiments across various domains such as images, tabular data, speech, and graphs. Our results show that the proposed method improves Mixup across various datasets using a variety of architectures, for instance, exhibiting an improvement over Mixup by 0.8% in ImageNet top-1 accuracy.

1 INTRODUCTION

Deep Neural Networks (DNNs) represent a class of very powerful function approximators, and large-scale DNNs have achieved state-of-the-art performance in many application areas such as computer vision (Krizhevsky et al., 2012), natural language understanding (Devlin et al., 2018), speech recognition (Hinton et al., 2012), reinforcement learning (Silver et al., 2016), and natural sciences (Jumper et al., 2021). In a supervised learning setting, typically, DNNs are trained to minimize their average error on the training samples. This training principle is known as Empirical Risk Minimization (ERM) (Vapnik, 1998).

Although being a simple training principle, training neural networks with ERM have a major problem: in the absence

of regularization techniques, instead of learning meaningful concepts, neural networks trained with ERM are prone to *memorize* training data (Arpit et al., 2017). This results in poor generalization to test samples, which come from a distribution slightly different from the training samples. To address this limitation of ERM, recently Mixup (Zhang et al., 2018) has been proposed as an alternative training principle. In a nutshell, instead of training a neural network on individual samples and their corresponding outputs, Mixup trains a neural network on the linear interpolation of the samples and the corresponding linear interpolation of the outputs.

Mathematically, let us suppose that x_i and x_j are input vectors corresponding to two randomly drawn samples i and j from the training distribution, and y_i and y_j are their one-hot encoded labels. Then, Mixup constructs a training sample as $\tilde{x} = \lambda x_i + (1 - \lambda)x_j$ and $\tilde{y} = \lambda y_i + (1 - \lambda)y_j$, where $\lambda \in [0, 1]$. Training with this kind of synthetic samples encourages the model to learn a function where linear interpolation in the input vectors leads to the linear interpolation of the corresponding targets. This kind of constraint limits the model complexity, and thus limits their ability to memorize training samples. Mixup can be interpreted as a data-agnostic *data augmentation* technique that does not require expert knowledge for creating additional training samples. Mixup can also be interpreted from the viewpoint of *Vicinal Risk Minimization* (VRM) principle (Chapelle et al., 2000). In this view, Mixup proposes a generic vicinal distribution based on the interpolation of training samples and their associated targets, and the additional training samples are drawn from such vicinal distribution around each training sample (Zhang et al., 2018).

Despite its simplicity and minimal computation overhead, Mixup and its variants have been shown to achieve state-of-the-art in many tasks such as, but not limited to, image classification (Yun et al., 2019; Kim et al., 2020; Faramarzi et al., 2020), object detection (Jeong et al., 2021), speech recognition (Lam et al., 2020; Tomashenko et al., 2018), text classification (Guo et al., 2019; Zhang et al., 2020), and medical image segmentation (Panfilov et al., 2019). Recently, Mixup was theoretically analyzed and shown to be

approximately equivalent to adding a second-order regularization term to the standard loss function (Zhang et al., 2021). However, if the benefit of Mixup can be explained by a second-order regularization, the following natural question arises: why we cannot replace Mixup with the second-order regularization?

In this paper, we show that Mixup cannot be replaced by the second-order regularization because Mixup is equivalent to adding infinitely many regularization terms on the directional derivatives of all orders instead of only the second order. Based on this novel insight, instead of replacing Mixup with a regularizer, this paper proposes to explicitly enhance the implicit regularization effect of Mixup on the directional derivatives. We name this method as *MixupE* (Mixup Enhanced). Figure 1 shows the training and test loss of ERM, Mixup, and *MixupE* on CIFAR-100 dataset trained with Wide-Resnet-28-10 (Zagoruyko and Komodakis, 2016) architecture. We can see that *MixupE* has higher training loss, implying that it works as a stronger regularizer than Mixup and ERM. This subsequently results in having better generalization (lower test loss) than Mixup and ERM.

To understand the benefits of *MixupE* empirically, we conduct experiments on a variety of datasets, such as images, tabular data and speech data, using various architectures such as LeNet (LeCun et al., 1998), VGG (Simonyan and Zisserman, 2014), ResNet (He et al., 2016), Vision Transformer (ViT, Dosovitskiy et al., 2020), and CoAtNet (Dai et al., 2021). In our experiments, we consistently see the *MixupE* has better generalization error than Mixup and ERM.

2 METHODS

In this section, we derive our method with a new mathematical understanding of Mixup. We begin in Section 2.1 with the notation used to present our theory and method. Mixup is then shown to implicitly regularize infinitely many directional derivatives of all orders in Section 2.2. Using this theoretical insight, we conclude that we cannot replace Mixup with an explicit regularizer, but we can enhance the regularization effect on the directional derivatives. In Section 2.3, we present our method to strengthen the regularization effect of Mixup based on a theoretical derivation.

2.1 Notation

We denote by $z = (x, y)$ the input and output pair where $x \in \mathcal{X} \subseteq \mathbb{R}^d$ and $y \in \mathcal{Y} \subseteq \mathbb{R}^D$. We define $f_\theta(x) \in \mathbb{R}^D$ to be the output of the logits (i.e., the last layer before the softmax or sigmoid) of the model parameterized by θ . We use $l(\theta, z)$ to denote the loss: for example, $l(\theta, z) = -\log \frac{\exp(y^\top f_\theta(x))}{\sum_k \exp(f_\theta(x)_k)}$ for the cross-entropy loss with $y \in \{0, 1\}^D$ being a one-hot vector, and $l(\theta, z) = -\log \frac{\exp(y f_\theta(x))}{1 + \exp(f_\theta(x))}$ for the logistic

loss with $y \in \{0, 1\}$. Let g be the softmax function for the cross-entropy loss, and the sigmoid function for the logistic loss.

Given a training dataset $S = ((x_i, y_i))_{i=1}^n$ of size n with $x_i \in \mathcal{X}$ and $y_i \in \mathcal{Y}$, we define the Mixup version of the input and output pair by $\tilde{z}_{i,j}(\lambda) = (\tilde{x}_{i,j}(\lambda), \tilde{y}_{i,j}(\lambda))$ where $\tilde{x}_{i,j}(\lambda) = \lambda x_i + (1 - \lambda)x_j$ and $\tilde{y}_{i,j}(\lambda) = \lambda y_i + (1 - \lambda)y_j$ with the Mixup coefficient $\lambda \in [0, 1]$. Then, we denote the standard empirical loss by $L_n^{std}(\theta, S) = \frac{1}{n} \sum_{i=1}^n l(\theta, z_i)$ and the Mixup loss by $L_n^{mix}(\theta, S) = \frac{1}{n^2} \sum_{i,j=1}^n \mathbb{E}_{\lambda \sim \text{Beta}(\alpha, \beta)} l(\theta, \tilde{z}_{ij}(\lambda))$ where $\text{Beta}(\alpha, \beta)$ represents the beta distribution with its parameters $\alpha, \beta > 0$. We let $a_\lambda = 1 - \lambda$ and $[n] = \{1, \dots, n\}$.

We define a mixture of beta distributions as $\mathcal{D}_\lambda = \frac{\alpha}{\alpha + \beta} \text{Beta}(\alpha + 1, \beta) + \frac{\beta}{\alpha + \beta} \text{Beta}(\beta + 1, \alpha)$; i.e., a sample with this distribution is drawn with probabilities $\frac{\alpha}{\alpha + \beta}$ and $\frac{\beta}{\alpha + \beta}$ from $\text{Beta}(\alpha + 1, \beta)$ and $\text{Beta}(\beta + 1, \alpha)$ respectively. For any function φ and point $u \in \mathbb{R}^d$ in its domain with $\varphi(u) \in \mathbb{R}^D$, we denote the matrix containing its j -th order derivatives by $\partial^j \varphi(u) \in \mathbb{R}^{D \times d^j}$ with each entry $\partial^j \varphi(u)_{k,i} = \text{vec}[T^{(k)}]_i$ where $T^{(k)}$ is the j -th order tensor $T_{i_1 i_2 \dots i_j}^{(k)} = \frac{\partial^j}{\partial u_{i_1} \partial u_{i_2} \dots \partial u_{i_j}} \varphi(u)_k$ and $\text{vec}[T^{(k)}] \in \mathbb{R}^{d^j}$ is the vectorization of the tensor. For example, $\partial^1 \varphi(u)$ is the Jacobian of φ evaluated at u . For an vector $a \in \mathbb{R}^d$, we define $a^{\otimes j} = a \otimes a \otimes \dots \otimes a \in \mathbb{R}^{d^j}$ where \otimes represents the Kronecker product. Finally, we let \mathcal{D}_X be the empirical distribution of the given training dataset (x_1, \dots, x_n) .

2.2 Motivation and Derivation via Theoretical Understanding

The following theorem shows that Mixup induces the regularization on j -th order directional derivatives of the model f_θ in the direction of $\mathbb{E}_{\tilde{x} \sim \mathcal{D}_X} [(\tilde{x} - x_i)^{\otimes j}]$ for all orders $j \in \mathbb{N}_+$:

Theorem 1. *Let l represent the cross-entropy loss or the logistic loss; i.e., $l(\theta, z) = -\log \frac{\exp(y^\top f_\theta(x))}{\sum_k \exp(f_\theta(x)_k)}$ or $l(\theta, z) = -\log \frac{\exp(y f_\theta(x))}{1 + \exp(f_\theta(x))}$. Define h such that $h(z) = \log(\sum_k \exp(z_k))$ if l represents the cross-entropy loss, and $h(z) = \log(1 + \exp(z))$ otherwise. Then, for any $J \in \mathbb{N}_+$, if f_θ is J -times differentiable at x_i for $i \in [n]$, there exists functions ψ and ψ_i such that $\lim_{a \rightarrow 0} \psi(a) = 0$, $\lim_{a \rightarrow 0} \psi_i(a) = 0$, and*

$$L_n^{mix}(\theta, S) = L_n^{std}(\theta, S) + \frac{1}{n} \sum_{i=1}^n \mathbb{E}_{\lambda \sim \mathcal{D}_\lambda} \mathbb{E}_{\tilde{x} \sim \mathcal{D}_X} \left(\sum_{j=1}^J \frac{a_\lambda^j}{j!} \partial^j h(f_\theta(x_i)) \Delta_i^{\otimes j} - a_\lambda y_i^\top \Delta_i + a_\lambda^J \psi(a_\lambda) \right),$$

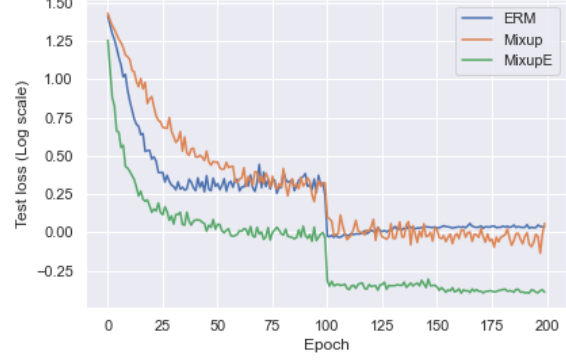
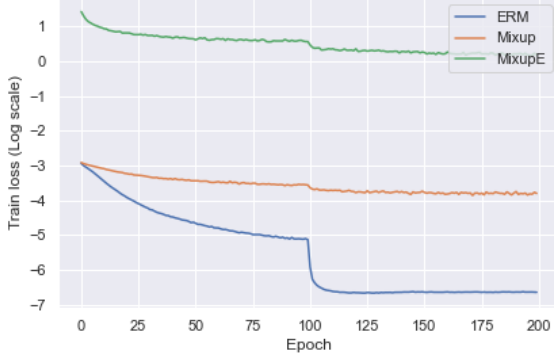


Figure 1: Comparison of train and test loss of ERM, Mixup, and *MixupE*. We see that *MixupE* has higher training loss but better test loss than Mixup and ERM.

where $\partial h(f_\theta(x_i)) = g(f_\theta(x_i))^\top \in \mathbb{R}^{1 \times D}$, and

$$\Delta_i = \sum_{j=1}^J \frac{a_\lambda^{j-1}}{j!} \partial^j f_\theta(x_i) (\bar{x} - x_i)^{\otimes j} + a_\lambda^{J-1} \psi_i(a_\lambda).$$

The proof of Theorem 1 is given in Appendix 1. Theorem 1 provides the following novel insight: while we can understand Mixup through the induced regularizer, we cannot replace Mixup with the explicit computation of the regularizer, because it involves infinitely many directional derivatives of all orders $j \in \mathbb{N}_+$. In other words, Mixup is an efficient closed-form solution to *implicitly* regularize infinitely many directional derivatives of all orders. Therefore, it is expected to be beneficial to keep Mixup instead of replacing it with the corresponding regularizer.

In this view, Theorem 1 provides a theoretical motivation to further improve Mixup by enhancing the regularization effect of Mixup on the directional derivatives. For the computational efficiency, we propose to strengthen the first-order term while letting Mixup implicitly take care of the higher order terms. In Theorem 1, the regularization effect of Mixup on the first-order directional derivatives is captured by $\frac{\mathbb{E}_{\lambda \sim \mathcal{D}_\lambda} [a_\lambda]}{n} \sum_{i=1}^n q(x_i)$, where

$$q(x_i) = (g(f_\theta(x_i)) - y_i)^\top \partial f_\theta(x_i) (\mathbb{E}_{\bar{x} \sim \mathcal{D}_X} [\bar{x}] - x_i), \quad (1)$$

and $\partial f_\theta(x_i) \in \mathbb{R}^{D \times d}$. Here, $q(x_i)$ can be approximated by

$$\bar{q}(x_i) = (y_i - g(f_\theta(x_i)))^\top f_\theta(x_i), \quad (2)$$

without computing the derivatives of f_θ explicitly. This is because $q(x_i) = \bar{q}(x_i)$ if $\mathbb{E}_{\bar{x} \sim \mathcal{D}_X} [\bar{x}] = 0$ (which can be ensured via the normalization of the training dataset) and $\partial f_\theta(x_i)x_i = f_\theta(x_i)$ (which can be ensured by using deep neural networks with ReLU activations). Thus, we have $q(x_i) \approx \bar{q}(x_i)$ if $\mathbb{E}_{\bar{x} \sim \mathcal{D}_X} [\bar{x}] \approx 0$ and $\partial f_\theta(x_i)x_i \approx f_\theta(x_i)$, which is the case in many common problems.

However, there is an issue of the implicit regularization on the first-order derivative via Mixup. From the definition of q above, we can rewrite it as

$$q(x_i) = \sum_{k=1}^D \alpha_{k,i} \|\partial f_k(x_i)\|_2 \|\mathbb{E}_{\bar{x} \sim \mathcal{D}_X} [\bar{x}] - x_i\|_2 \quad (3)$$

where $f_k(x_i)$ is the k -th coordinate of $f(x_i)$, $\alpha_{k,i} = (g(f_k(x_i)) - y_i)_k \zeta_{k,i}$, and $\zeta_{k,i}$ is the cosine similarity of two vectors $\partial f_k(x_i)$ and $\mathbb{E}_{\bar{x} \sim \mathcal{D}_X} [\bar{x}] - x_i$. Here, if α_k is positive, then Mixup tends to minimize the first-order derivative $\|\partial f_k(x_i)\|_2$ as desired. However, if α_k is negative, Mixup has an unintended effect of maximizing $\|\partial f_k(x_i)\|_2$. Figure 2 shows that the values of α_k are negative for some sample x_i and coordinate k in the initial phase of Mixup training. We show these values for both Preactresnet18 and Preactresnet50 architectures on CIFAR10 dataset.

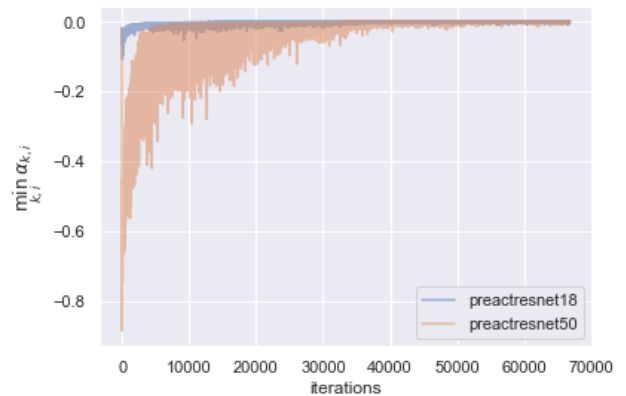


Figure 2: Minimum value of α over the coordinate k and sample i for different iterations during the training.

2.3 Proposed Algorithm

To avoid the unintended effect of maximizing $\|\partial f_k(x_i)\|_2$ in the initial phase of Mixup training, the proposed method

```

def beta_mean(alpha, beta):
    return alpha / (alpha + beta)

lam_mod_mean = beta_mean(alpha + 1, alpha) # mean of beta distribution

# y1, y2 should be one-hot vectors
for (x1, y1), (x2, y2) in zip(loader1, loader2):
    lam = numpy.random.beta(alpha, alpha)
    x = Variable(lam * x1 + (1. - lam) * x2)
    y = Variable(lam * y1 + (1. - lam) * y2)
    loss = loss_function(net(x), y) # mixup loss
    loss_scale = torch.abs(loss.detach().data.clone())
    f = net(x1)
    b = y1 - torch.softmax(f, dim=1)
    loss_new = torch.sum(f * b, dim=1)
    loss_new = (1.0 - lam_mod_mean) * torch.sum(torch.abs(loss_new)) / batch_size #
    additional loss term
    loss = loss + (mixup_eta * loss_new) # total loss
    loss_new_scale = torch.abs(loss.detach().data.clone())
    loss = (loss_scale / loss_new_scale) * loss # loss after scaling
    optimizer.zero_grad()
    loss.backward()
    optimizer.step()

```

Listing 1: One epoch *MixupE* training in PyTorch

adds the following term to the original loss while using Mixup:

$$R(\theta) = \frac{\mathbb{E}_{\lambda \sim \mathcal{D}_\lambda}[a_\lambda]}{n} \sum_{i=1}^n |\tilde{q}(x_i)|, \quad (4)$$

where $\tilde{q} = q$ for the accurate version and $\tilde{q} = \bar{q}$ for the approximate version. The functions q and \bar{q} are defined in equations (1) and (2). The approximate version does not require computation of the directional derivatives and the computational cost is negligible because $f_\theta(x_i)$ is already computed for the original loss and the value of $\mathbb{E}_{\lambda \sim \mathcal{D}_\lambda}[a_\lambda]$ does not change over epoch: e.g., $\mathbb{E}_{\lambda \sim \mathcal{D}_\lambda}[a_\lambda] = 1 - \frac{\alpha+1}{2\alpha+1}$ when $\text{Beta}(\alpha, \alpha)$ is used for Mixup. In general, we have that $R(\theta) \rightarrow 0$ as $\alpha, \beta \rightarrow 0$ when $\text{Beta}(\alpha, \beta)$ is used for Mixup. In other words, as Mixup gets closer to ERM without Mixup (i.e., $\alpha, \beta \rightarrow 0$), the additional term $R(\theta)$ vanishes.

In addition, we scale the magnitude of the entire loss back to that of the original loss so that the improvement is not an artifact of the additional magnitude of the loss. That is, by letting $\mathcal{L}(\theta)$ be the original loss, our method uses the following loss:

$$\tilde{\mathcal{L}}(\theta) = \kappa (\mathcal{L}(\theta) + \eta R(\theta)), \quad (5)$$

where $\kappa = \frac{|\mathcal{L}(\theta)|}{|\mathcal{L}(\theta) + \eta R(\theta)|}$ is detached from the computational graph so that the gradient does not go through the κ . Here, $\eta > 0$ is the only hyperparameter of the proposed method.

In Listing 1, we show a code block for *MixupE*: extending Mixup to *MixupE* requires one additional forward pass on the *original* (non-mixed) sample for computing the additional loss term and requires one additional hyperparameter η in comparison to Mixup.

We note that the code block in Listing 1 shows how to apply *MixupE* when the training sample is in the form of a fixed shape tensor (for example, images, tabular data). For applying *MixupE* to training samples that have irregular (not fixed) topology, such as graphs, sequences, and trees, as the first step, we need to project the input samples to a fixed shape hidden states using an encoder network, after this step, *MixupE* can be applied in the usual form.

3 EXPERIMENTS

We present a range of experiments to back up the methodological claims, demonstrate versatility across benchmark problems, and show practical applicability on images, tabular data, and speech problems.

3.1 Image Datasets

For small-scale image datasets, we consider CIFAR-10, CIFAR-100, SVHN, and Tiny-ImageNet. We run our experiments using a variety of architectures including PreActResNet18, PreActResNet34, PreActResNet50, PreActResNet101 (He et al., 2016), and Wide-Resnet-28-10 (Zagoruyko and Komodakis, 2016).

Throughout our experiments, we use SGD+Momentum optimizer with batch-size 100, learning rate 0.1, momentum 0.9 and weight-decay 10^{-4} , with step-wise learning rate decay. We train all the networks for all the datasets for 200 epochs and the learning rate is annealed by a factor of 10 at epochs 100 and 150.

Hyperparameters α and η : For Mixup on CIFAR-10

Table 1: Classification errors on (a) CIFAR-10 and (b) CIFAR-100. Standard deviations over five repetitions. Best performing methods in **bold**.

(a) CIFAR-10		(b) CIFAR-100	
PreActResNet50	Test Error (%)	PreActResNet50	Test Error (%)
ERM	4.71 \pm 0.062	ERM	24.68 \pm 0.349
Mixup	4.53 \pm 0.041	Mixup	23.03 \pm 0.471
<i>MixupE</i>	3.53 \pm 0.047	<i>MixupE</i>	20.23 \pm 0.507
PreActResNet101		PreActResNet101	
ERM	4.21 \pm 0.069	ERM	23.20 \pm 0.362
Mixup	4.43 \pm 0.049	Mixup	23.05 \pm 0.383
<i>MixupE</i>	3.35 \pm 0.049	<i>MixupE</i>	18.86 \pm 0.376
Wide-Resnet-28-10		Wide-Resnet-28-10	
ERM	4.24 \pm 0.101	ERM	22.20 \pm 0.108
Mixup	3.03 \pm 0.091	Mixup	19.38 \pm 0.113
<i>MixupE</i>	2.94 \pm 0.048	<i>MixupE</i>	17.12 \pm 0.111

and CIFAR-100 datasets, we used the value $\alpha = 1.0$ as recommended in Zhang et al. (2018). For Mixup on SVHN and Tiny-ImageNet datasets, we experimented with the α values 1.0 and 0.2 respectively as recommended in Verma et al. (2019a). We experimented with the $\eta \in \{0.0001, 0.001, 0.01, 0.1\}$, and obtained the best results using $\eta = 0.001$ for most of the experiments, and using $\eta = 0.0001$ for the remaining experiments.

Results: We show results for the CIFAR-10 (Table 1a), CIFAR-100 (Table 1b), SVHN (Table 2a), and Tiny-ImageNet (Table 2b) datasets. We see that *MixupE* consistently outperforms baseline methods ERM and Mixup across all the datasets and architectures.

Sensitivity to hyperparameter η : To validate that the method is not overly sensitive to the newly introduced hyperparameter η , we conducted experiments for *MixupE* with the value of $\eta \in \{0.0001, 0.001, 0.01, 0.1\}$ with Preactresnet50 architecture and CIFAR100 dataset. This experiment was repeated five times with different initializations. We got the mean test error (in %) of 20.23, 20.84, 21.01, 20.87 for the η values of 0.0001, 0.001, 0.01, 0.1, respectively, vs the mean test-error 23.03 for Mixup. This suggests that the proposed method *MixupE* is not overly sensitive to the hyperparameter η and works better than Mixup for a large range of η values.

For a large-scale image classification dataset, we consider ImageNet (Deng et al., 2009), using three architectures: ResNet (He et al., 2016), Vision Transformer (ViT, Dosovitskiy et al., 2020), and CoAtNet (Dai et al., 2021). In particular, we use ResNet-50, ViT-B/16, and CoAtNet-0. We choose these architectures for experiments because they are fast to train, and they respectively represent the three families of image classification models: convolution-based

models, attention-based models, and hybrid models.

Except for the Mixup-related hyperparameters α and η , all training hyperparameters for these models follow their original paper. Specifically, all models are trained and evaluated at the resolution of 224x224. Our ResNet-50 is trained with a SGD+Momentum with the momentum coefficient of 0.9, while our ViT-B/16 and CoAtNet-0 are both trained with AdamW (Loshchilov and Hutter, 2018), $\beta_1 = 0.9$ and $\beta_2 = 0.99$. An L_2 weight decay of 10^{-4} is applied to our ResNet-50, while the larger weight decays of 0.05 and 0.3 are applied to our CoAtNet-0 and ViT-B/16, respectively.

All models were trained for 100K steps, with a global batch size of 4096. Throughout these 100K training steps, the learning rate starts from 0 and warms up linearly to its peak value – which is 1.6 for ResNet-50 and 0.001 for ViT and CoAtNet – and then decreases to 1/1000 times the peak value following the cosine schedule. For models with batch normalization, i.e., ResNet-50 and CoAtNet-0, the batch statistics during training are computed globally. We also apply a Polyak moving average with the rate of 0.999 on all parameters, *including* the batch normalization cumulative statistics in the case of ResNet-50 and CoAtNet-0.

Hyperparameters α and η : we use the Mixup rate $\alpha = 0.2$ for ResNet-50, following the suggestions from Zhang et al. (2018). Since ViT-B/16 and CoAtNet-0 were invented after Mixup, we first tune the value of α and found that $\alpha = 0.4$ offers a sweet spot for these models. Fixing $\alpha = 0.2$ for ResNet-50 and $\alpha = 0.4$ for ViT-B/16 and CoAtNet-0, we then tune the values for η with ResNet-50. We find that $\eta = 10^{-3}$ is best for ResNet-50 while the smaller value of $\eta = 5 \times 10^{-4}$ is best for ViT-B/16 and CoAtNet-0.

ImageNet results: Table 3 presents our results. We ob-

Table 2: Classification error on SVHN and classification accuracy on Tiny-Imagenet. Standard deviations over five repetitions. Best performing methods in **bold**.

(a) Classification Error on SVHN		(b) Classification Accuracy on Tiny-ImageNet		
PreActResNet50	Test Error (%)	PreActResNet18	top-1	top-5
ERM	4.71 \pm 0.062	ERM	54.97 \pm 0.52	72.71 \pm 0.48
Mixup	4.53 \pm 0.041	Mixup	54.64 \pm 0.43	72.53 \pm 0.51
<i>MixupE</i>	3.53 \pm 0.047	<i>MixupE</i>	62.21 \pm 0.39	82.09 \pm 0.41
PreActResNet101		PreActResNet34		
ERM	4.21 \pm 0.069	ERM	57.25 \pm 0.48	72.58 \pm 0.53
Mixup	4.43 \pm 0.049	Mixup	57.79 \pm 0.39	76.15 \pm 0.42
<i>MixupE</i>	3.35 \pm 0.049	<i>MixupE</i>	65.37 \pm 0.31	83.77 \pm 0.35
Wide-Resnet-28-10		PreActResNet50		
ERM	4.24 \pm 0.101	ERM	55.91 \pm 0.61	73.50 \pm 0.57
Mixup	3.03 \pm 0.091	Mixup	54.86 \pm 0.46	73.11 \pm 0.43
<i>MixupE</i>	2.94 \pm 0.048	<i>MixupE</i>	67.22 \pm 0.38	85.14 \pm 0.36

serve that *MixupE* consistently outperforms Mixup across the three architectures in our experiments. Notably, the gains of *MixupE* – in terms of top-1 accuracy – are larger for ViT-B/16 and CoAtNet-0 than for ResNet-50, *i.e.* +0.7 and +0.8 compared to +0.5, even though the top-1 accuracy of the Mixup baselines for ViT-B/16 and CoAtNet-0 are higher. We note that other extensions of Mixup, such as CutMix (Yun et al., 2019), PuzzleMix (Kim et al., 2020), and PatchUp (Faramarzi et al., 2020) use *non-linear* mixing of samples, thus they are not directly comparable with *MixupE*. We leave an experimental comparison of *MixupE* with these methods using a common implementation scheme (architecture and training/validation protocol) as a future work.

Table 3: ImageNet accuracy of various models. Each experiment was run for 3 times.

Models	MixUp Type	Top-1	Top-5
ResNet-50	None	76.2 \pm 0.5	93.6 \pm 0.3
	MixUp	77.2 \pm 0.2	94.0 \pm 0.1
	<i>MixupE</i>	77.7 \pm 0.2	94.4 \pm 0.1
ViT-B/16	None	79.1 \pm 0.2	95.1 \pm 0.1
	MixUp	79.7 \pm 0.2	95.4 \pm 0.1
	<i>MixupE</i>	80.4 \pm 0.1	95.8 \pm 0.1
CoAtNet-0	None	79.8 \pm 0.2	95.1 \pm 0.1
	MixUp	80.8 \pm 0.3	95.5 \pm 0.1
	<i>MixupE</i>	81.6 \pm 0.2	95.7 \pm 0.2

A note on implementation and runtime. Despite these improvements, *MixupE* requires twice as many forward passes as compared to normal Mixup. As shown in Listing 1, the extra computation stems from the forward pass through the original (non-mixed) samples, *i.e.* $f = \text{net}(x_1)$. For

larger models running on ImageNet, this cost can lead to significantly slower experiment time. To alleviate the experiment time, we “batch” this extra pass through the non-mixup data into the pass through the mixup data. Thanks to this trick, our implementation of *MixupE* is only 1.3 times slower than Mixup.

3.2 Tabular Datasets

We consider a number of tabular environments drawn from the UCI dataset (Lichman et al., 2013), namely *Arrhythmia*, *Letter*, *Balance-scale*, *Mfeat-factors*, *Mfeat-fourier*, *Mfeat-karhunen*, *Mfeat-morphological*, *Mfeat-zernike*, *CMC*, *Optdigits*, *Pendigits*, *Iris*, *Mnist_784*, *Abalone* and *Volkert*.

We consider the same setting as Zhang et al. (2018) where the network is a fully-connected multi-layer perceptron (MLP) with two hidden layers, each with 128 dimensions, with ReLU activations for non-linearity. We train this network with the Adam optimizer using the cross-entropy loss with the default learning rate of 0.001 and a batch size of 100, for 25 epochs. We feed in the categorical part of the data as one-hot inputs, and for any samples with missing features in the dataset, we fill it with the mean (for continuous) or mode (for discrete) of those features.

Hyperparameters α and η : We consider the hyper-parameters from the set $\alpha \in \{0.01, 0.02, 0.05, 0.1, 0.2, 0.5, 1.0, 2.0, 5.0\}$ and $\eta \in \{0.0001, 0.001, 0.01, 0.1, 1.0\}$ and run five seeds for each of the combinations and algorithms. Then, the value of (α, η) is chosen based on the best validation accuracy, corresponding to which we report the test accuracy for that particular dataset.

Results: Table 4 presents our results for a subset of the

Table 4: Classification Test Error (%) on tabular datasets from UCI repository. Results are averaged over five trials.

Dataset	Method		
	ERM	Mixup	<i>MixupE</i>
Arrhythmia	34.60 ± 3.10	35.49 ± 3.88	34.85 ± 3.99
Letter	4.56 ± 0.27	3.71 ± 0.18	4.04 ± 0.20
Balance-scale	3.87 ± 1.03	3.70 ± 1.00	3.68 ± 0.97
Mfeat-factors	2.74 ± 0.81	2.44 ± 0.42	2.56 ± 0.64
Mfeat-fourier	17.69 ± 1.76	17.80 ± 1.56	17.57 ± 1.60
Mfeat-karhunen	3.74 ± 0.58	3.06 ± 0.29	2.47 ± 0.32
Mfeat-morph	25.00 ± 2.10	24.62 ± 1.83	24.66 ± 1.30
Mfeat-zernike	17.58 ± 1.72	15.19 ± 1.73	15.55 ± 0.62
CMC	45.77 ± 1.49	46.67 ± 1.83	45.42 ± 2.05
Optdigits	1.48 ± 0.19	1.15 ± 0.21	1.33 ± 0.14
Pendigits	1.03 ± 0.25	0.76 ± 0.19	0.72 ± 0.16
Iris	9.06 ± 7.01	8.14 ± 6.48	7.29 ± 6.95
Mnist_784	2.83 ± 0.11	2.57 ± 0.05	2.56 ± 0.14
Abalone	35.05 ± 0.61	35.07 ± 0.69	34.91 ± 0.70
Volkert	33.26 ± 0.62	32.74 ± 0.76	32.54 ± 0.61

tabular datasets (see appendix) for results on all datasets). We observe that *MixupE* outperforms the standard Mixup as well as ERM across multiple datasets.

3.3 Speech Dataset

To have a rigorous comparison with (Zhang et al., 2018), similar to their work, for speech dataset we use Google commands dataset (Warden, 2018). This dataset consists of 65000 one-second long utterances of 30 short words such as *yes, no, up, down, left, right, stop, go, on, off*, by thousands of different people. 30 short words correspond to 30 classes. We preprocess the utterances by first extracting the normalized spectrograms from the original waveform at a sampling rate of 16 kHz, followed by zero-padding the spectrograms to equalize their size at 160×101 . This preprocessing step is exactly same as (Zhang et al., 2018). Furthermore, similar to (Zhang et al., 2018), we use LeNet (LeCun et al., 1998) and VGG-11 and VGG-13 (Simonyan and Zisserman, 2014) architectures. We train all the models for 20 epochs using Adam optimizer with a learning rate of 0.001 and batch-size of 100.

Hyperparameters α and η : For all the architectures, we first find the best value of hyperparameter α for Mixup from the set $\alpha \in \{0.1, 0.2, 0.5, 1.0, 2.0\}$. We observed that $\alpha = 0.2$ works best consistently for all architectures. For *MixupE*, we used the best α values from Mixup, and only fine-tuned the η hyperparameter using

Table 5: Classification Test Error (%) on Google Speech Command Dataset (Warden, 2018). We run each experiment five times

Architecture	Method		
	ERM	Mixup	<i>MixupE</i>
LeNet	10.43 ± 0.052	10.12 ± 0.041	10.02 ± 0.042
VGG-11	6.04 ± 0.059	4.63 ± 0.047	3.93 ± 0.050
VGG-13	5.77 ± 0.053	4.68 ± 0.039	3.84 ± 0.040

$\eta \in \{0.001, 0.01, 0.1, 1.0\}$. In our experiments $\eta = 0.01$ works best for all the experiments.

Results: In Table 5, we observe that *MixupE* improves the test error of Mixup for different architectures. Moreover, the improvement is more significant for larger architectures such as VGG-11 and VGG-13 than LeNet.

3.4 Graph Datasets

For graph classification, we consider the *MUTAG*, *NC11*, *PTC*, *PROTEINS*, *IMDB-BINARY* and *IMDB-MULTI* datasets. We use the experimental settings defined in (Xu et al., 2018) as the baseline system, where Mixup and *MixupE* is performed after encoding the graph to a fixed dimensional vector, that is, at the graph-level readout stage. Each system here relies on 5 graph neural network layers that give rise to the readout, which is then operated on by a non-linear MLP. The models are trained for 350 epochs using Adam optimizer with a learning rate of 0.01, which is halved every 50 epochs. For the hyperparameters, we consider $\alpha \in \{0.01, 0.02, 0.05, 0.1, 0.2, 0.5, 1.0, 2.0, 5.0\}$ and $\eta \in \{0.0001, 0.001, 0.01, 0.1, 1.0\}$. Corresponding to each model setting, we perform 10-fold validation and identify which epoch and hyperparameters give the best test accuracy, and report the final mean and standard deviation of the algorithm on it over the ten folds. We refer the readers to Table 6, which shows the benefits of using *MixupE* on the graph datasets.

3.5 Ablation Experiments

In *MixupE*, we have proposed to add an additional loss term derived from the first-order derivative (4) to the Mixup Loss 5. A natural question arises: what would be the performance of adding this term to the ERM loss? We conduct an ablation study to investigate this question. Specifically, we compare the following four methods : 1) ERM, 2) Mixup, 3) ERM+additional loss, 4) Mixup+additional loss (*MixupE*). The test error on CIFAR100 dataset using the Preactresnet50 architecture for the above mentioned method is shown in Table 7.

Results in Table 7 show that adding the additional loss term

Table 6: Classification Test Error (%) on graph datasets from the TUDatasets benchmark when following the setup of Xu et al. (2018). Results are obtained from 10-fold validation.

Dataset	Method		
	ERM	Mixup	<i>MixupE</i>
MUTAG	10.15 \pm 0.06	10.67 \pm 0.05	10.06 \pm 0.06
NC11	17.79 \pm 0.02	18.59 \pm 0.02	17.74 \pm 0.01
PTC	38.37 \pm 0.09	34.87 \pm 0.08	35.50 \pm 0.08
PROTEINS	25.43 \pm 0.04	24.44 \pm 0.04	23.72 \pm 0.04
IMDBBINARY	25.60 \pm 0.03	25.30 \pm 0.03	25.20 \pm 0.03
IMDBMULTI	50.33 \pm 0.03	49.27 \pm 0.04	48.53 \pm 0.03

Table 7: Ablation experiments to understand the effect of the additional loss term in Equation 4. Each experiment was run for 5 times.

Method	Test Error
ERM	24.68
Mixup	23.03
ERM+additional loss	22.42
Mixup+additional loss (<i>MixupE</i>)	20.23

of Equation 4 improves the test accuracy in Mixup. This is consistent with our argument in Section 2.2 that Mixup can have an unintended effect of maximizing $\|\partial f_k(x_i)\|_2$. Furthermore, we observe that Mixup+additional loss (*MixupE*) performs better than ERM+additional loss; this indicates that the implicit regularization of higher order directional derivative through Mixup training is important for better test errors, thus justifying our proposed method.

4 RELATED WORK

Mixup (Zhang et al., 2018; Tokozume et al., 2017) and its numerous variants have seen remarkable success in supervised learning problems, as well as other problems such as semi-supervised learning (Verma et al., 2021a; Berthelot et al., 2019), unsupervised learning using autoencoders (Beckham et al., 2019; Berthelot* et al., 2019), adversarial learning (Lamb et al., 2019; Lee et al., 2020; Pang* et al., 2020), graph-based learning (Verma et al., 2019b), computer vision (Yun et al., 2019; Jeong et al., 2021; Panfilov et al., 2019; Faramarzi et al., 2020), natural language (Guo et al., 2019; Zhang et al., 2020) and speech (Lam et al., 2020; Tomashenko et al., 2018).

Mixup (Zhang et al., 2018) creates synthetic training samples by linear interpolation in the input vectors and their corresponding labels. The follow-up work of Mixup can be categorized into two main categories: (a) methods that pro-

pose a *non-linear* interpolation in the input vector (or hidden vectors), examples of this category include (Yun et al., 2019; Faramarzi et al., 2020; Kim et al., 2020; Zhang et al., 2020; Verma et al., 2021b). (b) methods that extend linear interpolation based Mixup training to various learning paradigms or applications, examples of this class include Mixup based training for supervised learning (Verma et al., 2019a), semi-supervised learning (Verma et al., 2021a; Berthelot et al., 2019), for adversarial training (Lamb et al., 2019), for node classification (Verma et al., 2019b), and for natural language processing (Guo et al., 2019). The method proposed in this work can be applied to any of the methods in the latter category, and we leave experimental evaluation of *MixupE* applied to these methods for future work.

Theoretically, Mixup has been analyzed in Zhang et al. (2021) in which the authors show that it is approximately equivalent to adding a second-order regularizer to improve robustness and generalization. They did not propose a method based on the theory. In contrast, this paper shows that it is equivalent to adding infinite many regularization on the directional derivatives of all orders, and used this theory to propose a new method.

5 CONCLUSION AND LIMITATIONS

In this work, we have theoretically derived a new method to improve Mixup without using any domain-specific properties of the datasets. Our theory shows that Mixup is a computationally efficient way to regularize directional derivatives of all orders. Our method is mathematically designed to strengthen the regularization effect of Mixup. The proposed method *MixupE* outperforms Mixup on several datasets such as image, tabular, and speech datasets, trained with various networks. The improvement in test error is more significant for networks with larger capacity. As a limitation, our method requires one additional forward pass in the network during training than Mixup. Nevertheless, in Section 3.1, we show that the implementation of our method is only 1.3 times slower than Mixup. While we focused on the first-order term for the computational efficiency as a first step, our results suggest a promising future research direction to enhance Mixup by studying higher-order terms in Theorem 1. Moreover, Theorem 1 shows that we cannot fully understand Mixup only based on the second order term. This provides an open problem of understanding Mixup using all orders of the directional derivatives in Theorem 1.

References

- Arpit, D., Jastrzbski, S., Ballas, N., Krueger, D., Bengio, E., Kanwal, M. S., Maharaj, T., Fischer, A., Courville, A., Bengio, Y., et al. (2017). A closer look at memorization in deep networks. In *Proceedings of the International Conference on Machine Learning*, pages 233–242. PMLR.
- Beckham, C., Honari, S., Verma, V., Lamb, A. M., Ghadiri,

-
- F., Hjelm, R. D., Bengio, Y., and Pal, C. (2019). On adversarial mixup resynthesis. In *Advances in Neural Information Processing Systems*, volume 32, pages 4346–4357. Curran Associates, Inc.
- Berthelot, D., Carlini, N., Goodfellow, I., Papernot, N., Oliver, A., and Raffel, C. (2019). MixMatch: A Holistic Approach to Semi-Supervised Learning. *arXiv e-prints*, page arXiv:1905.02249.
- Berthelot*, D., Raffel*, C., Roy, A., and Goodfellow, I. (2019). Understanding and improving interpolation in autoencoders via an adversarial regularizer. In *International Conference on Learning Representations*.
- Chapelle, O., Weston, J., Bottou, L., and Vapnik, V. (2000). Vicinal risk minimization. *Advances in Neural Information Processing Systems*, 13.
- Dai, Z., Liu, H., Le, Q. V., and Tan, M. (2021). Coatnet: Marrying convolution and attention for all data sizes. *Advances in Neural Information Processing Systems*, 34:3965–3977.
- Deng, J., Dong, W., Socher, R., Li, L.-J., Li, K., and Fei-Fei, L. (2009). Imagenet: A large-scale hierarchical image database. In *Proceedings of the IEEE Conference on Computer Vision and Pattern Recognition*, pages 248–255. IEEE.
- Devlin, J., Chang, M.-W., Lee, K., and Toutanova, K. (2018). Bert: Pre-training of deep bidirectional transformers for language understanding. *arXiv preprint arXiv:1810.04805*.
- Dosovitskiy, A., Beyer, L., Kolesnikov, A., Weissenborn, D., Zhai, X., Unterthiner, T., Dehghani, M., Minderer, M., Heigold, G., Gelly, S., et al. (2020). An image is worth 16x16 words: Transformers for image recognition at scale. *arXiv preprint arXiv:2010.11929*.
- Faramarzi, M., Amini, M., Badrinaaraayanan, A., Verma, V., and Chandar, S. (2020). Patchup: A regularization technique for convolutional neural networks. *arXiv preprint arXiv:2006.07794*.
- Guo, H., Mao, Y., and Zhang, R. (2019). Augmenting data with mixup for sentence classification: An empirical study. *arXiv preprint arXiv:1905.08941*.
- He, K., Zhang, X., Ren, S., and Sun, J. (2016). Deep residual learning for image recognition. In *Proceedings of the IEEE Conference on Computer Vision and Pattern Recognition*, pages 770–778.
- Hinton, G., Deng, L., Yu, D., Dahl, G. E., Mohamed, A.-r., Jaitly, N., Senior, A., Vanhoucke, V., Nguyen, P., Sainath, T. N., et al. (2012). Deep neural networks for acoustic modeling in speech recognition: The shared views of four research groups. *IEEE Signal Processing Magazine*, 29(6):82–97.
- Jeong, J., Verma, V., Hyun, M., Kannala, J., and Kwak, N. (2021). Interpolation-based semi-supervised learning for object detection. In *Proceedings of the IEEE/CVF Conference on Computer Vision and Pattern Recognition*, pages 11602–11611.
- Jumper, J., Evans, R., Pritzel, A., Green, T., Figurnov, M., Ronneberger, O., Tunyasuvunakool, K., Bates, R., Zidek, A., Potapenko, A., Bridgland, A., Meyer, C., Kohl, S. A. A., Ballard, A. J., Cowie, A., Romera-Paredes, B., Nikolov, S., Jain, R., Adler, J., Back, T., Petersen, S., Reiman, D., Clancy, E., Zielinski, M., Steinegger, M., Pacholska, M., Berghammer, T., Bodenstern, S., Silver, D., Vinyals, O., Senior, A. W., Kavukcuoglu, K., Kohli, P., and Hassabis, D. (2021). Highly accurate protein structure prediction with AlphaFold. *Nature*, 596(7873):583–589.
- Kim, J.-H., Choo, W., and Song, H. O. (2020). Puzzle mix: Exploiting saliency and local statistics for optimal mixup. In *Proceedings of the International Conference on Machine Learning*, pages 5275–5285. PMLR.
- Krizhevsky, A., Sutskever, I., and Hinton, G. E. (2012). Imagenet classification with deep convolutional neural networks. *Advances in Neural Information Processing Systems*, 25.
- Lam, M. W. Y., Wang, J., Su, D., and Yu, D. (2020). Mixup-breakdown: A consistency training method for improving generalization of speech separation models. In *International Conference on Acoustics, Speech and Signal Processing (ICASSP)*, pages 6374–6378.
- Lamb, A., Verma, V., Kannala, J., and Bengio, Y. (2019). Interpolated adversarial training: Achieving robust neural networks without sacrificing too much accuracy. In *Proceedings of the 12th ACM Workshop on Artificial Intelligence and Security, AISEc’19*, page 95–103, New York, NY, USA. Association for Computing Machinery.
- LeCun, Y., Bottou, L., Bengio, Y., and Haffner, P. (1998). Gradient-based learning applied to document recognition. In *Proceedings of the IEEE*, volume 86, pages 2278–2324.
- Lee, S., Lee, H., and Yoon, S. (2020). Adversarial vertex mixup: Toward better adversarially robust generalization. *Proceedings of the IEEE/CVF Conference on Computer Vision and Pattern Recognition*, pages 269–278.
- Lichman, M. et al. (2013). UCI machine learning repository.
- Loshchilov, I. and Hutter, F. (2018). Decoupled weight decay regularization. In *International Conference on Learning Representations*.
- Panfilov, E., Tiulpin, A., Klein, S., Nieminen, M. T., and Saarakkala, S. (2019). Improving robustness of deep learning based knee MRI segmentation: Mixup and adversarial domain adaptation. In *Proceedings of the IEEE/CVF International Conference on Computer Vision Workshops*.

-
- Pang*, T., Xu*, K., and Zhu, J. (2020). Mixup inference: Better exploiting mixup to defend adversarial attacks. In *International Conference on Learning Representations*.
- Silver, D., Huang, A., Maddison, C. J., Guez, A., Sifre, L., Van Den Driessche, G., Schrittwieser, J., Antonoglou, I., Panneershelvam, V., Lanctot, M., et al. (2016). Mastering the game of go with deep neural networks and tree search. *Nature*, 529(7587):484–489.
- Simonyan, K. and Zisserman, A. (2014). Very deep convolutional networks for large-scale image recognition. *arXiv preprint arXiv:1409.1556*.
- Tokozume, Y., Ushiku, Y., and Harada, T. (2017). Between-class learning for image classification. *Proceedings of the IEEE/CVF Conference on Computer Vision and Pattern Recognition*, pages 5486–5494.
- Tomashenko, N., Khokhlov, Y., and Estève, Y. (2018). Speaker adaptive training and mixup regularization for neural network acoustic models in automatic speech recognition. In *Proceedings of Interspeech*, pages 2414–2418.
- Vapnick, V. N. (1998). *Statistical Learning Theory*. Wiley, New York.
- Verma, V., Lamb, A., Beckham, C., Najafi, A., Mitliagkas, I., Lopez-Paz, D., and Bengio, Y. (2019a). Manifold mixup: Better representations by interpolating hidden states. In *Proceedings of the 36th International Conference on Machine Learning*, pages 6438–6447.
- Verma, V., Lamb, A., Juho, K., Bengio, Y., and Lopez-Paz, D. (2021a). Interpolation consistency training for semi-supervised learning. In Kraus, S., editor, *Proceedings of the Twenty-Eighth International Joint Conference on Artificial Intelligence (IJCAI)*.
- Verma, V., Luong, T., Kawaguchi, K., Pham, H., and Le, Q. (2021b). Towards domain-agnostic contrastive learning. In *Proceedings of the International Conference on Machine Learning*, pages 10530–10541. PMLR.
- Verma, V., Qu, M., Kawaguchi, K., Lamb, A., Bengio, Y., Kannala, J., and Tang, J. (2019b). Graphmix: Improved training of gnns for semi-supervised learning. *arXiv preprint arXiv:1909.11715*.
- Warden, P. (2018). Speech commands: A dataset for limited-vocabulary speech recognition. *arXiv preprint arXiv:1804.03209*.
- Xu, K., Hu, W., Leskovec, J., and Jegelka, S. (2018). How powerful are graph neural networks? *arXiv preprint arXiv:1810.00826*.
- Yun, S., Han, D., Oh, S. J., Chun, S., Choe, J., and Yoo, Y. (2019). Cutmix: Regularization strategy to train strong classifiers with localizable features. In *Proceedings of the IEEE/CVF international conference on computer vision*, pages 6023–6032.
- Zagoruyko, S. and Komodakis, N. (2016). Wide residual networks. *arXiv preprint arXiv:1605.07146*.
- Zhang, H., Cisse, M., Dauphin, Y. N., and Lopez-Paz, D. (2018). mixup: Beyond empirical risk minimization. In *International Conference on Learning Representations*.
- Zhang, L., Deng, Z., and Kawaguchi, K. (2021). How does mixup help with robustness and generalization? In *International Conference on Learning Representations (ICLR)*.
- Zhang, R., Yu, Y., and Zhang, C. (2020). SeqMix: Augmenting active sequence labeling via sequence mixup. *arXiv preprint arXiv:2010.02322*.

Supplementary Material for MixupE

6 Proof of Theorem 1

Proof. For the cross-entropy loss, we have

$$l(\theta, (x, y)) = -\log \frac{\exp(y^\top f_\theta(x))}{\sum_k \exp(f_\theta(x)_k)} = \log \left(\sum_k \exp(f_\theta(x)_k) \right) - y^\top f_\theta(x)$$

where $y \in \mathbb{R}^D$ is a one-hot vector. For the logistic loss,

$$l(\theta, (x, y)) = -\log \frac{\exp(y f_\theta(x))}{1 + \exp(f_\theta(x))} = \log(1 + \exp(f_\theta(x)) - y f_\theta(x)).$$

Thus, for both cases, we can write

$$l(\theta, (x, y)) = h(f_\theta(x)) - y^\top f_\theta(x).$$

where $h(z) = \log(\sum_k \exp(z_k))$ for the cross-entropy loss and $h(z) = \log(1 + \exp(z))$ for the logistic loss. Using this and equation (9) of (Zhang et al., 2021), we have that

$$L_n^{\text{mix}}(\theta, S) = \frac{1}{n} \sum_{i=1}^n \mathbb{E}_{\lambda \sim \mathcal{D}_\lambda} \mathbb{E}_{\tilde{x} \sim \mathcal{D}_X} l(\theta, (\tilde{x}_i, y_i)),$$

where \mathcal{D}_X is the empirical distribution induced by training samples, and

$$\tilde{x}_i = \lambda x_i + (1 - \lambda)\bar{x}.$$

Define $a = 1 - \lambda$. Then,

$$\tilde{x}_i = (1 - a)x_i + a\bar{x} = x_i + a(\bar{x} - x_i).$$

Define

$$\varphi_i(a) = f_\theta(x_i + a(\bar{x} - x_i)).$$

If f_θ is J -times differentiable at x_i , then by definition of the differentiability, there exists a function ψ_i such that $\lim_{a \rightarrow 0} \psi_{i, \bar{x}}(a) = 0$ and

$$\varphi_i(a) = \varphi_i(0) + \sum_{j=1}^J \frac{a^j}{j!} \varphi_i^{(j)}(0) + a^J \psi_i(a) = f_\theta(x_i) + \sum_{j=1}^J \frac{a^j}{j!} \varphi_i^{(j)}(0) + a^J \psi_{i, \bar{x}}(a),$$

where $\varphi_i^{(j)}(0)$ is the j -th order derivative of φ_i at 0. Here, for any $j \in \mathbb{N}^+$, by defining $b = x_i \in \mathbb{R}^d$,

$$\varphi_i^{(j)}(0) = \sum_{k_1=1}^d \sum_{k_2=1}^d \cdots \sum_{k_j=1}^d \frac{\partial^j f_\theta(b)}{\partial b_{k_1} \partial b_{k_2} \cdots \partial b_{k_j}} (\bar{x} - x_i)_{k_1} (\bar{x} - x_i)_{k_2} \cdots (\bar{x} - x_i)_{k_j}.$$

Then, by using the vectorization of the tensor $\partial^j f_\theta(b) \in \mathbb{R}^{D \times d^j}$, we can rewrite this equation as

$$\varphi_i^{(j)}(0) = \partial^j f_\theta(x_i) (\bar{x} - x_i)^{\otimes j}, \tag{6}$$

where $(\bar{x} - x_i)^{\otimes j} = (\bar{x} - x_i) \otimes (\bar{x} - x_i) \otimes \cdots \otimes (\bar{x} - x_i) \in \mathbb{R}^{d^j}$. Summarising above, there exists a function $\psi_{i,\bar{x}}$ such that $\lim_{a \rightarrow 0} \psi_{i,\bar{x}}(a) = 0$ and

$$f_\theta(x_i + a(\bar{x} - x_i)) = f_\theta(x_i) + \sum_{j=1}^J \frac{a^j}{j!} \partial^j f_\theta(x_i) (\bar{x} - x_i)^{\otimes j} + a^J \psi_{i,\bar{x}}(a).$$

By defining $\Delta_i = \sum_{j=1}^J \frac{a^{j-1}}{j!} \partial^j f_\theta(x_i) (\bar{x} - x_i)^{\otimes j} + a^{J-1} \psi_{i,\bar{x}}(a)$, we have that

$$\begin{aligned} l(\theta, (\check{x}_i, y_i)) &= l(\theta, (x_i + a(\bar{x} - x_i), y_i)) \\ &= h(f_\theta(x_i + a(\bar{x} - x_i))) - y_i^\top f_\theta(x_i + a(\bar{x} - x_i)) \\ &= h(f_\theta(x_i) + a\Delta_i) - y_i^\top (f_\theta(x_i) + a\Delta_i). \end{aligned}$$

Similarly, by defining $\varphi'_i(a) = h(f_\theta(x_i) + a\Delta_i)$, there exists a function $\psi'_{i,\bar{x}}$ such that $\lim_{a \rightarrow 0} \psi'_{i,\bar{x}}(a) = 0$ and

$$h(f_\theta(x_i) + a\Delta_i) = h(f_\theta(x_i)) + \sum_{j=1}^J \frac{a^j}{j!} \partial^j h(f_\theta(x_i)) \Delta_i^{\otimes j} + a^J \psi'_{i,\bar{x}}(a).$$

Combining these,

$$\begin{aligned} l(\theta, (\check{x}_i, y_i)) &= h(f_\theta(x_i)) - y_i^\top f_\theta(x_i) - a y_i^\top \Delta_i + \sum_{j=1}^J \frac{a^j}{j!} \partial^j h(f_\theta(x_i)) \Delta_i^{\otimes j} + a^J \psi'_{i,\bar{x}}(a) \\ &= l(\theta, (x_i, y_i)) - a y_i^\top \Delta_i + \sum_{j=1}^J \frac{a^j}{j!} \partial^j h(f_\theta(x_i)) \Delta_i^{\otimes j} + a^J \psi'_{i,\bar{x}}(a). \end{aligned}$$

Thus, by writing $a_\lambda = 1 - \lambda$ to make the dependence clear,

$$\begin{aligned} L_n^{\text{mix}}(\theta, S) &= \frac{1}{n} \sum_{i=1}^n \mathbb{E}_{\lambda \sim \mathcal{D}_\lambda} \mathbb{E}_{\bar{x} \sim \mathcal{D}_X} l(\theta, (\check{x}_i, y_i)) \\ &= L_n^{\text{std}}(\theta, S) + \frac{1}{n} \sum_{i=1}^n \mathbb{E}_{\lambda \sim \mathcal{D}_\lambda} \mathbb{E}_{\bar{x} \sim \mathcal{D}_X} \left(\sum_{j=1}^J \frac{a_\lambda^j}{j!} \partial^j h(f_\theta(x_i)) \Delta_i^{\otimes j} - a_\lambda y_i^\top \Delta_i + a_\lambda^J \psi'_{i,\bar{x}}(a_\lambda) \right), \end{aligned}$$

where

$$\Delta_i = \sum_{j=1}^J \frac{a_\lambda^{j-1}}{j!} \partial^j f_\theta(x_i) (\bar{x} - x_i)^{\otimes j} + a_\lambda^{J-1} \psi_{i,\bar{x}}(a_\lambda).$$

Since $\lim_{\alpha \rightarrow 0} \frac{1}{n} \sum_{i=1}^n \mathbb{E}_{\bar{x} \sim \mathcal{D}_X} \psi'_{i,\bar{x}}(a) = 0$ and $\lim_{\alpha \rightarrow 0} \mathbb{E}_{\bar{x} \sim \mathcal{D}_X} \psi_{i,\bar{x}}(a) = 0$, there exists functions ψ and ψ_i such that $\lim_{a \rightarrow 0} \psi(a) = 0$, $\lim_{a \rightarrow 0} \psi_i(a) = 0$, and

$$\begin{aligned} L_n^{\text{mix}}(\theta, S) &= L_n^{\text{std}}(\theta, S) + \frac{1}{n} \sum_{i=1}^n \mathbb{E}_{\lambda \sim \mathcal{D}_\lambda} \mathbb{E}_{\bar{x} \sim \mathcal{D}_X} \left(\sum_{j=1}^J \frac{a_\lambda^j}{j!} \partial^j h(f_\theta(x_i)) \Delta_i^{\otimes j} - a_\lambda y_i^\top \Delta_i + a_\lambda^J \psi(a_\lambda) \right), \end{aligned}$$

where

$$\Delta_i = \sum_{j=1}^J \frac{a_\lambda^{j-1}}{j!} \partial^j f_\theta(x_i) (\bar{x} - x_i)^{\otimes j} + a_\lambda^{J-1} \psi_i(a_\lambda).$$

Finally, we compute $\partial h(f_\theta(x_i))$. Recall that $h(z) = \log(\sum_k \exp(z_k))$ for the cross-entropy loss and $h(z) = \log(1 + \exp(z))$ for the logistic. For the cross-entropy loss, we have $\frac{\partial h(z)}{\partial z_t} = (\sum_k \exp(z_k))^{-1} \exp(z_t) = g(z)_t$, where g is the softmax function. Similarly, for the logistic loss, since $h(z) = \log(1 + \exp(z))$, we have that $\frac{\partial h(z)}{\partial z} = (1 + \exp(z))^{-1} \exp(z) = g(z)$, where g is the sigmoid function. Therefore, for both cases of the cross-entropy loss and the logistic loss, we have that $\partial h(f_\theta(x_i)) = g(f_\theta(x_i))^\top \in \mathbb{R}^{1 \times D}$.

□